Civil Engineering Infrastructures Journal 2022, 55(1): 31-41
DOI: 10.22059/CEIJ.2021.306156.1690

TECHNICAL NOTE

Development of the Fragility Curves for Conventional Reinforced Concrete Moment Resistant Frame Structures in Qods Town, Qom City, Iran

Dehghani, E.[1*] and Soltanimohajer, M.[2]

[1] Associate Professor, Faculty of Civil Engineering, University of Qom, Qom, Iran.
[2] M.Sc. Student, Faculty of Civil Engineering, University of Qom, Qom, Iran.

Received: 13 Jul. 2020; Revised: 24 Jan. 2021; Accepted: 30 Jan. 2021

ABSTRACT: In the Second World Conference on Disaster Risk Reduction (WCDRR) the concept of resilience has been presented as an Effective Strategy to improve post-earthquake conditions. One of the principles of resilience is "quick response", which requires having relevant information to determine the level of vulnerability of the city. For this purpose, many studies have been done in recent years to investigate the seismic behavior of a variety of infrastructures in a city. The fragility curve is one of the most popular tools among researchers to investigate the probabilistic seismic behavior of structures. It expresses the degree of structural vulnerability by indicating the exceedance probability of damage versus the given level of ground shaking. In this study, 24 fragility curves are developed for four typical intermediate Reinforced Concrete Moment Resistant Frame structures in Qods town (located in Qom, Iran) with two number of stories (4 and 8) and two number of bays (1 and 2). They are derived through nonlinear incremental dynamic analysis in one and two horizontal directions under two sets of near-field and far-field ground motion records. The results indicate that the seismic response of structures is the same for uni-directional and bi-directional analyses. Also, it seems that the response of the structures with periods greater than 1 sec is in correlation with the mass-to-stiffness ratio. Change in the width and number of bays of the structure does not affect the probability of failure, as far as the width to the number of bays ratio remains constant. Furthermore, the probability of failure is higher when the structure is subjected to near-field earthquake ground motion records.

Keywords: Damage Evaluation, Fragility Curve, Incremental Dynamic Analysis, Reinforced Concrete Moment Resistant Frame, SAP2000.

1. Introduction

Most of Iran's densely populated areas, which are located in the Alpine-Himalayan belt of China and a pressure zone due to the convergence of the two plates of Saudi Arabia and Eurasia, are considered as active tectonic zones. The occurrence of major earthquakes in the history of seismicity in these areas has made Iran the sixth most earthquake-prone country in the world (Taghizade et al., 2009).

The past experiences from these devastating earthquakes show that one of the important factors in the extent of the damage in these events is the lack of

* Corresponding author E-mail: dehghani@qom.ac.ir

sufficient information on the level of damage and how it is distributed throughout the city in the early hours, which delays the initial measures and interferes with crisis management.

Seismic risk assessment of different types of structures in a city provides the necessary information to estimate the damage and its distribution throughout the city. It can increase the resilience of the city by reducing the time of reaction to earthquakes, better management of outreach capacities, and reduction of damage. To do this, various methods for calculating seismic risk have been developed by the American Council on Applied Technology (ATC-13, 1985) (Rojahn, 1985), the Peer Earthquake Engineering Research Center (PEER) (Cornell and Krawinkler, 2000; Moehle and Deierlein, 2004), the US Central Crisis Management Agency-National Institute of Building Sciences (FEMA-NIBS) (Whitman and et al.,1996). Among the proposed methods, fragility models have always been of interest to researchers and are considered as one of the effective tools in seismic risk assessment that are calculated and presented in different ways.

In recent years, several studies have been conducted in this field in Iran. Ahmadi-Pa zoki et al. (2015) evaluated the fragility curves of the 3 and 6-story steel braced-frame buildings with and without infill panels for three levels of damage including Immediate Occupancy (IO), Life Safety (LS), and Collapse Prevention (CP). The probable damages and the related costs were estimated by using engineering economics methods in cost-benefit analysis, and the relationship between costs and damages for buildings with infill panel was proposed. Results showed that selecting a more appropriate limit state is more cost-efficient and the results are not sensitive to the minimum absorption rate and the structure's useful life.

Abdullahzadeh et al. (2015) investigated the seismic risk of a special truss moment-frame structure located in Tehran by developing fragility curves using the capacity spectrum method. The seismic hazard of the study area was described by using a reduced elastic response spectrum with a damping ratio of 5%. The results of this study showed that the special truss moment-frame with a Vierendeel middle panel suffered extensive damage due to buckling and early fracture of truss web members as well as special truss moment-frames with an X-diagonal middle members segment due to low seismic capacity.

Mohsenian et al. (2017) evaluated the seismic sensitivity of tunnel-form buildings with 5 and 10 stories to in-plan one-way mass eccentricity and determined the level of performance of the buildings under the design earthquake for various mass eccentricities.

Kouhestanian et al. (2019) developed the fragility curves of 3, 5, and 8-storey Reinforced Concrete Moment Resistant Frame structures with a soft and very soft-story under the main earthquake record and subsequent earthquakes, to investigate the effect of irregularity and aftershocks. The analysis results showed that the effect of irregularity and aftershocks on the seismic vulnerability of the 5 and 8-story structures was more pronounced than the 3-story structure.

Pahlavan et al. (2019) studied the seismic performance of low, medium, and high-rise reinforced concrete buildings located in the north of Iran. In their study, based on the results of previous field research, two structural deficiencies, including the reduced strength of concrete and insufficient overlap length of column's longitudinal bars were considered as common practical defects in the studied structures. The fragility curves of the models were derived through nonlinear incremental dynamic analysis under 20 far-field earthquake records. The models were also retrofitted with the conventional method of steel jacket of the columns and their seismic damage was determined for different functional levels. Comparison of the median values of seismic fragility of

models with structural weakness and retrofitted models showed that the median values of seismic fragility were significantly increased in the retrofitted models.

Mobinipour et al. (2020) investigated the influence of pulse-type of earthquake records on the fragility curves of the Steel Special Moment Resisting Frames (SMRFs). The results indicated that the median value of the collapse capacity due to near-fault ground motions was 76% that of the far-fault records for the ten-story example SMRF.

In this paper 24 fragility curves have been developed, with the aims of predicting the seismic performance of conventional concrete structures in Qods town of Qom city. They have been derived through nonlinear incremental dynamic analysis in one and two horizontal directions under two sets of near-field and far-field ground motion records. The geographical location of the case study region is shown in Figure 1.

2. Modeling

In this study, after conducting field investigations in Qods town, the Reinforced Concrete Moment Resistant Frame structure with intermediate ductility is chosen as the conventional residential building and is categorized into four groups:

- 4-story structure with a width of 6 meters (C406);
- 4-story structure with a width of 12 meters (C412);
- 8-story structure with a width of 6 meters (C806);
- 8-story structure with a width of 12 meters (C812).

The geometric characteristics of the case study structures are shown in Figure 2.

Due to the common construction practice adopted in this area, these structures are modeled in three dimensions using frame elements. The structures are designed based on the provisions of the fourth edition of the Iranian 2800 Code (BHRC, 2016) and ACI 318-14 (2014) specifications. The beam and column sections are determined between 30 and 60 cm in proportion and the ratio of longitudinal reinforcement has been calculated as 1 to 3% for columns and 0.35 to 1.5% for beams. The nonlinear behavior of materials is modeled by using concentrated plastic hinges in accordance with ASCE 41-13 (2014) specifications and the geometric nonlinearity of the structure (P-Delta) is considered by reducing the elements of the structure's stiffness matrix. The first and second natural period of vibration of each structure is reported in Table 1.

Fig. 1. Geographical location of the case study region

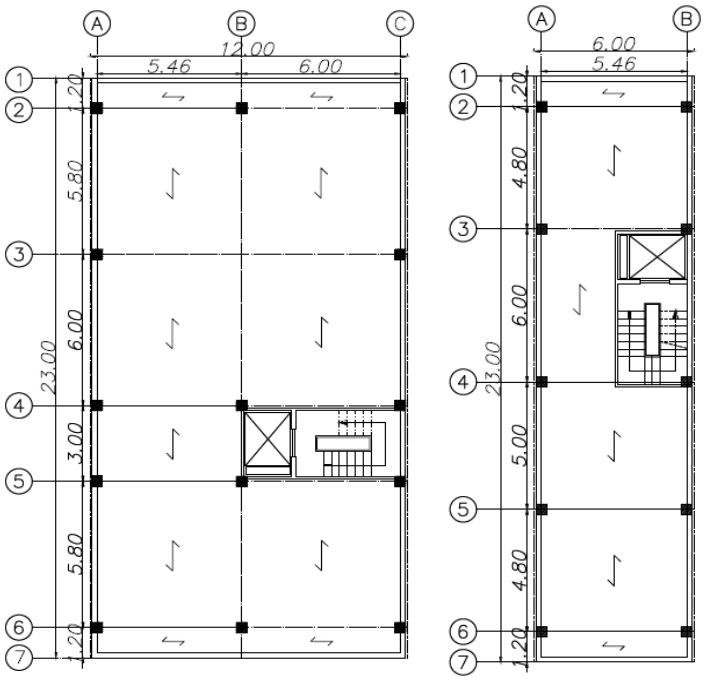

(a) **(b)**

Fig. 2. Geometric characteristics of the case study structures: a) Four- and eight-story structures with a width of 12 m; and b) Four- and eight-story structures with a width of 6 m

Table 1. Natural period of vibration of building models

Building model	First mode period (sec)	Second mode period (sec)
C812	1.97	1.93
C806	1.94	1.9
C412	1.4	1.2
C406	1.2	1.19

The structures are subjected to 28 near-field and 22 far-field earthquake ground motion records adopted from FEMA p695 (2009). Two sets of analysis are performed; in the first set, the structures are subjected to the selected records in one direction (transverse), and in the second set, they are analyzed in two perpendicular directions simultaneously using incremental dynamic analysis.

3. Development of Fragility Curve

In order to develop the fragility curve, the structure drift ratio (Figure 3) and the Peak Ground Acceleration (PGA) have been selected as the parameters describing the seismic behavior of the structure (Damage Measure) and the intensity of the ground motion (Intensity Measure), respectively. The hunt and fill algorithm has been employed to determine the intensity levels. The damage states are selected according to FEMA-356 (2006), IO, LS and CP. Structural performance levels and their corresponding damages for the concrete frame is reported in Table 2.

Table 2. Structural performance levels and damages for concrete frame (FEMA356, 2000)

Structural performance level	IO	LS	CP
Drift	1 %	2 %	4%

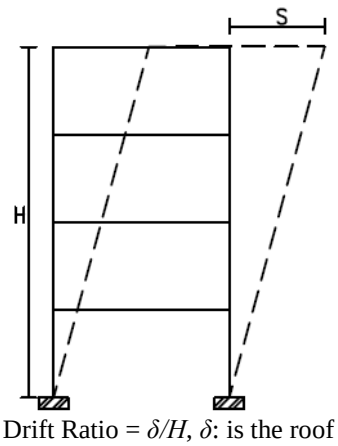

Fig. 3. Drift Ratio = δ/H, δ: is the roof relative displacement and H: is the height of the structure

The Lognormal Cumulative Distribution Function (CDF) is applied to the responses obtained from different records for a given seismic intensity to compute the probability of exceedance for each of the damage limit states as discrete. Finally, by using linear interpolation relationships, the fragility curve is obtained for each model. Eq. (1) shows the relationship between the fragility curve and the parameters used in this study.

$$\begin{aligned} &P[D \geq Ds_i \mid IM = im] = P[Drift \geq Drift(Ds_i) \mid PGA] \\ &= 1 - P[Drift \leq Drift(Ds_i) \mid PGA] \\ &= 1 - P\left[\Phi\left(\frac{Ln(Drift(Ds_i)) - \theta_d}{\beta_d}\right) \mid PGA\right] \end{aligned} \quad (1)$$

where P[*A* | *B*]: is the conditional probability of *A* given *B* occurs, *D*: describes the uncertainty in damage state, *IM*: is the intensity measure, *im*: is a particular value of *IM*, Ds_i: is the damage state (IO, LS, CP), *PGA*: varies between 0.005g and 3g (0.005, 0.055, …), $\Phi(s)$: is the standard normal cumulative distribution function, θ_d: is the mean natural logarithm of data, and β_d: is the standard deviation of the natural logarithm of data.

The software employed in this study is SAP2000, which has been augmented by the fragility curve code to perform incremental dynamic analysis.

4. Fragility Curve Code

In this study, the procedure of developing the fragility curve has been programmed in the MATLAB software. The "fragility curve code" algorithm is shown in Figure 4.

As can be seen in this figure, five parameters are received as input, including the initial step (S_0), the constant coefficient (S_x), the incremental coefficient (d_s), which are used to determine the intensity levels, and the height of the structure (*H*) and the node number (point name), which are used to extract the relative displacement of the user's desired points. Then, the SAP2000 software is opened and the model is called. The intensity levels are then determined using the hunt and fill algorithm and used to perform incremental dynamic analysis. The results of this part are saved in the response matrix and are used as the input of the fragility model in the next part. In the fragility model, the damage matrix is represented by the lognormal distribution and the user's desired performance levels. Finally, the response curve and the fragility curve are drawn as the output of the second and third parts of the fragility code, respectively.

5. Results

In this study, 24 fragility curves are derived for four typical intermediate Reinforced Concrete Moment Resistant Frame structures. The analysis is carried out in one and two horizontal directions under two sets of near-field and far-field ground motion records. The structures are coded as follows for reference: C406, C412, C806, and C812 respectively denote the 4-story structure with a width of 6 m, 4-story structure with a width of 12 m, 8-story structure with a width of 6 m, and 8-story structure with a width of 12 m. The near-field and far-field records are presented with suffixes NF and FF, respectively, and the direction of the analysis is indicated by X, XY, and YX. In order to distinguish between the curves for different analyses, the aforementioned suffixes are added to the code name of the structures (Figure 5).

6. Results of Bi-Directional Analysis

In order to investigate the simultaneous effect of longitudinal and transverse components of earthquake records on structural vulnerability and also to identify the more vulnerable direction, longitudinal and transverse fragility curves obtained from the bi-directional analysis are compared with the transverse fragility curve obtained from uni-directional analysis as shown in Figure 6.

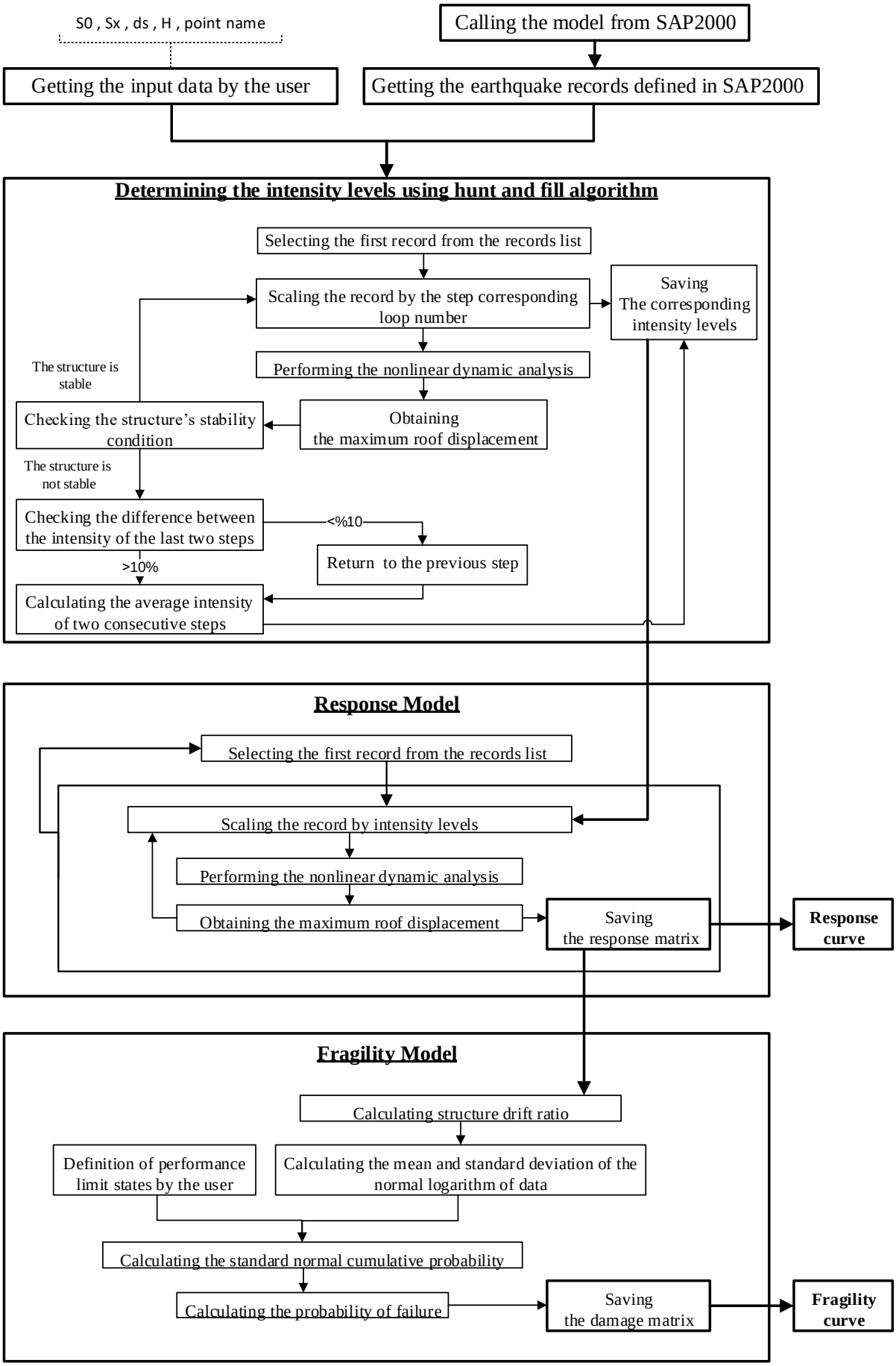

Fig. 4. Fragility curve code algorithm

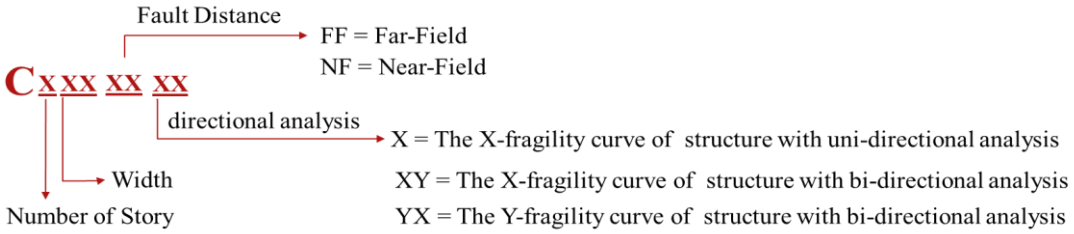

Fig. 5. Sample's Code

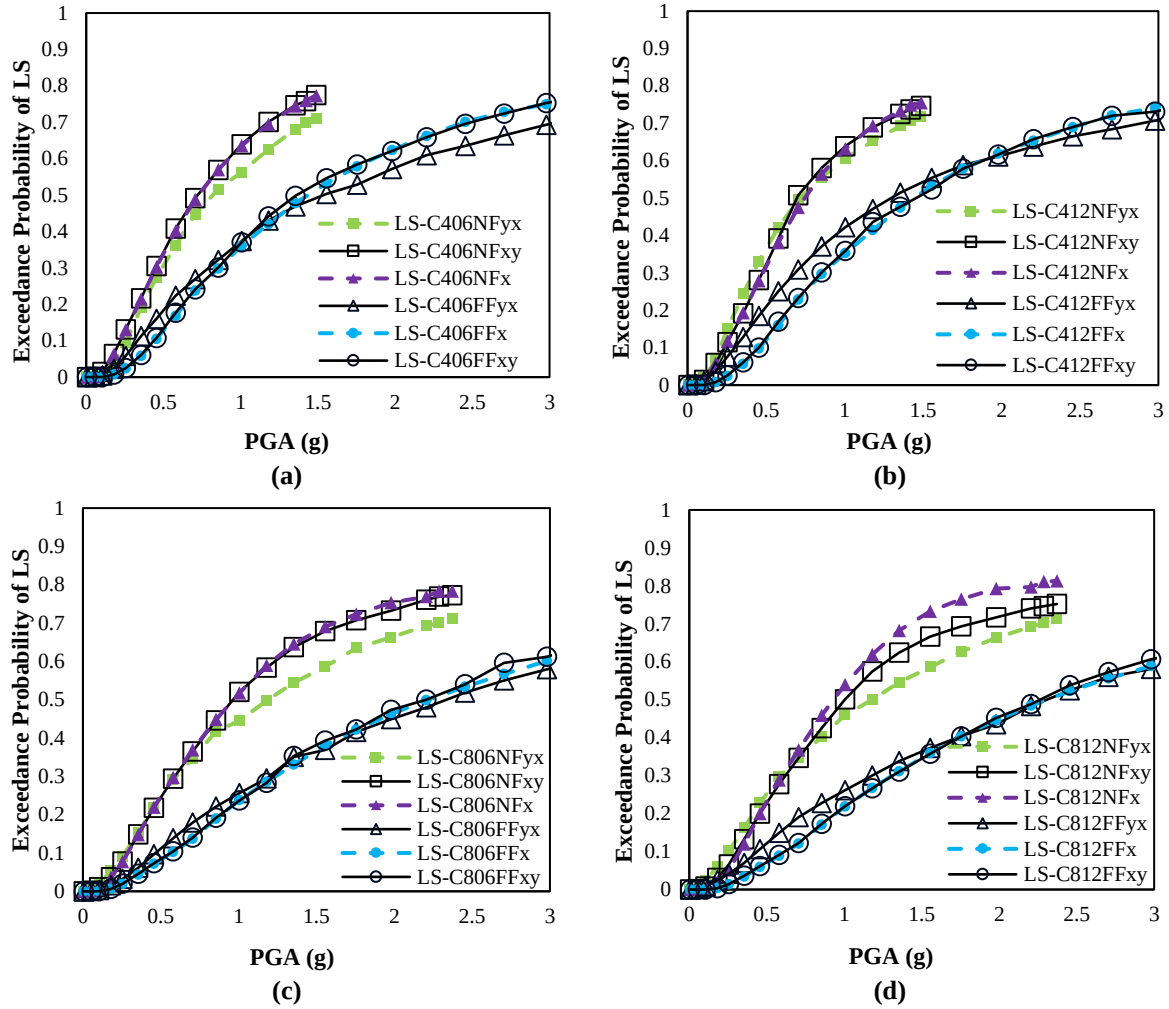

Fig. 6. Longitudinal and transverse fragility curves obtained from uni-directional and bi-directional analysis: a) C406; b) C412; c) C806; and d) C812

As can be observed in Figure 6, except for the fragility curve for model C812NF in which the difference between the results of the two analyses is less than 10%, it can be concluded that the results of the analyses for the case study structures, which comply to the regular structures as per 2800 standard code, are close to each other despite the 5% accidental torsion considered herein. Furthermore, the fragility curves obtained from the longitudinal and transverse direction analysis of the case study structures are very close to each other, though their difference increases with increasing intensity. In general, it can be stated that the damage probability is higher in the transverse direction. Therefore, the following evaluations in the paper are performed based on the fragility curve of the transverse direction resulting from the uni-directional analysis of structures.

7. Results of Uni-Directional Analysis

In this section, to investigate the effect of the width and height of the structure on their

vulnerability and also to identify the more destructive earthquakes, the fragility curve of the transverse direction of the structures under near-field and far-field earthquake records for three damage limit states, including IO, LS, and CP have been compared with each other.

As can be seen in Figure 7, the probability of failure of structures with different widths and number of bays, in which the ratio of the width of the structure to the number of bays is equal, is the same; in structures with different heights, the probability of failure of shorter structures is higher. Also, the probability of failure of structures subjected to near-field records is higher as compared to the far-field records.

In order to further examine the observations made in the above paragraph; the capacity curve of each structure is plotted using pushover analysis. The strength and stiffness of each structure are determined by using the equivalent bilinear curve whose slope of the first line and the area below it is equal to the initial slope and the area below their capacity curve, respectively. Note that, due to the unequal mass of the structures, the ratio of mass-to-strength and mass-to-stiffness are shown in Figure 8 for a better comparison.

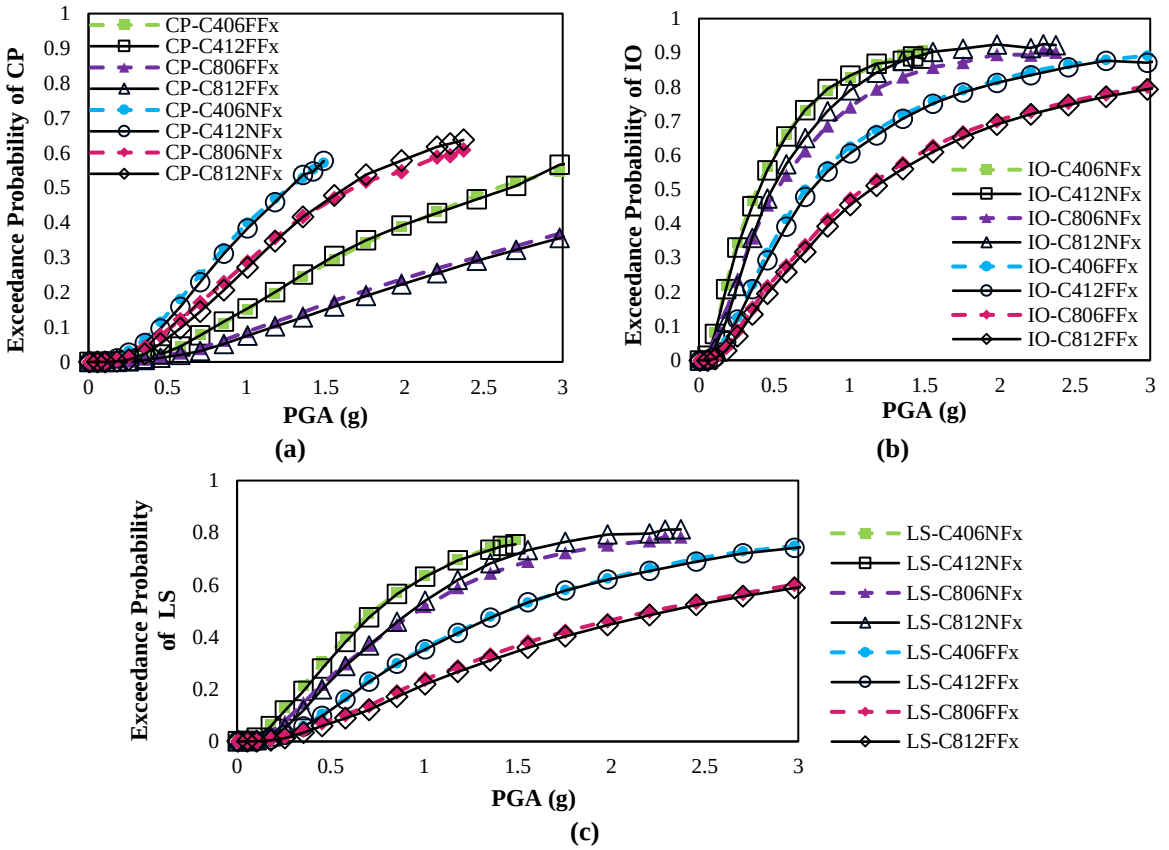

Fig. 7. Fragility curves in the transverse direction for the case study structures: a) exceedance probability for CP limit state; b) exceedance probability for IO limit state; and c) exceedance probability for LS limit state

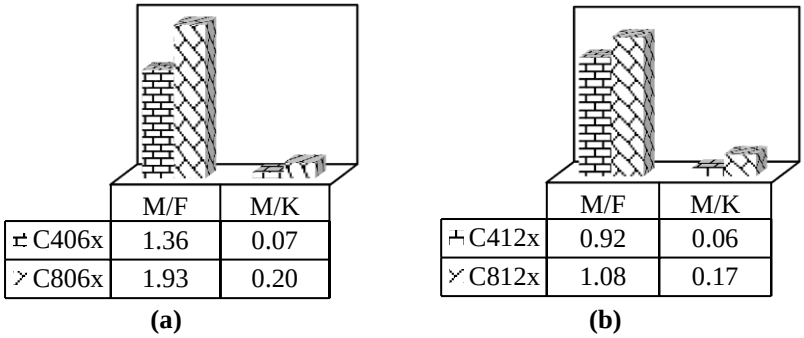

	M/F	M/K
C406x	1.36	0.07
C806x	1.93	0.20

(a)

	M/F	M/K
C412x	0.92	0.06
C812x	1.08	0.17

(b)

Fig. 8. Dynamic characteristics of the case study structures: a) C406 and C806; and b) C412 and C812

As can be observed in Figure 8, for structures of the same height and different widths, the mass-to-stiffness ratios are close to each other and the mass-to-strength ratio of the wider structures is smaller. Furthermore, in structures with the same width and different heights, the mass-to-stiffness and mass-to-strength of shorter structures are less.

By comparing the results of the fragility curve of the structures and their dynamic characteristics, it seems that the response of structures is determined based on the mass-to-stiffness ratio. Newmark et al. (1959) evaluated the seismic behavior of single-degree-of-freedom structures under nonlinear dynamic analysis and found out that for structures with periods greater than one second, the maximum displacement resulting from the linear and nonlinear analysis is equal. The probability of failure of shorter structures that have a lower mass-to-stiffness ratio can be justified by referring to the response spectrum of records used. The pseudo-velocity spectrum for near-field and far-field earthquake records are shown in Figure 9.

It is observed in Figure 9 that, approximately the range of period of vibration 0 to 4 seconds is an acceleration-sensitive region, 4 to 9 seconds is a velocity-sensitive region and 9 to 15 seconds is displacement sensitive region. Since the period of vibration of the structures studied in this paper is between 1 to 2 seconds, the pseudo-accelerations spectrum has been used to interpret the above observations. The pseudo- accelerations spectrum for near-field and far-field earthquake records are shown in Figure 10.

Figure 10 shows that, the shorter structures with a period of vibration of one second are subjected to bigger spectral accelerations than the taller structures with a period of vibration of two seconds.

8. Performance Evaluation of Case Study Structures Subjected to Seismic Excitation

In order to evaluate the seismic risk of Reinforced Concrete Moment Resistant Frame structures located in Qods town, the probability of failure for different damage limit states for a PGA of 0.3g, which is the design base acceleration of Qom city as per 2800 standard code, is presented in Figure 11.

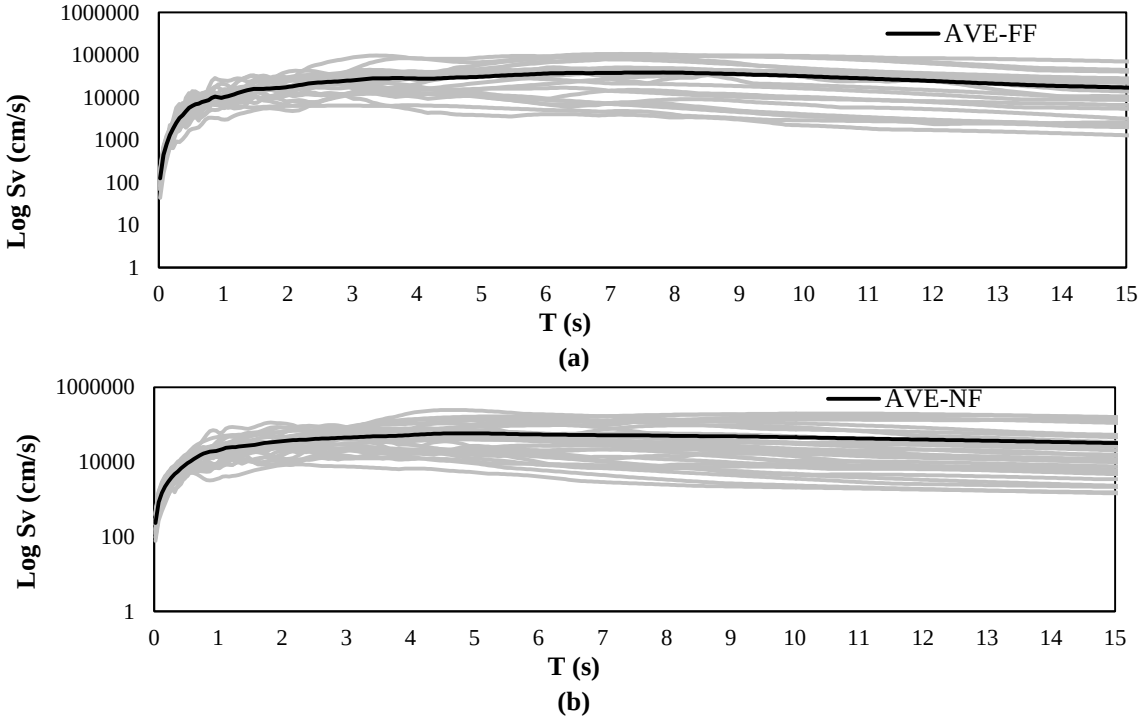

Fig. 9. Average pseudo-velocity spectrum for: a) near-field earthquake records; and b) far-field earthquake records

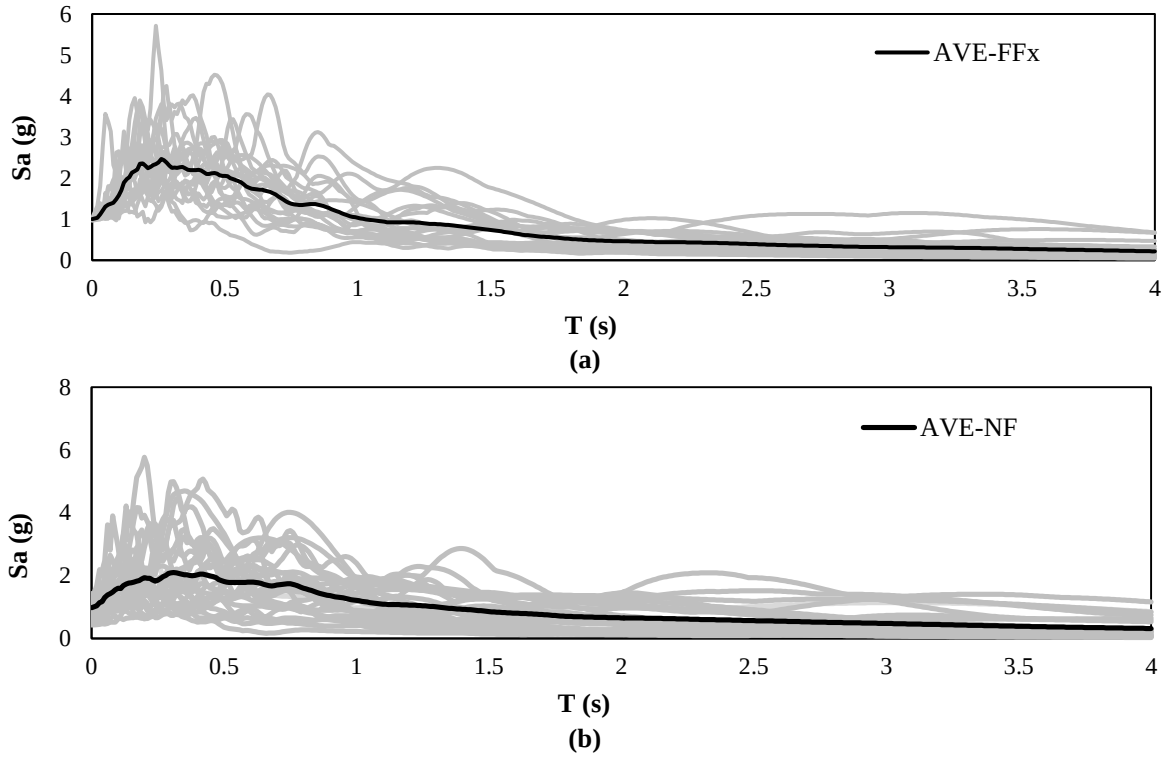

Fig. 10. Pseudo-accelerations spectrum for: a) far-field earthquake records; and b) near-field earthquake record

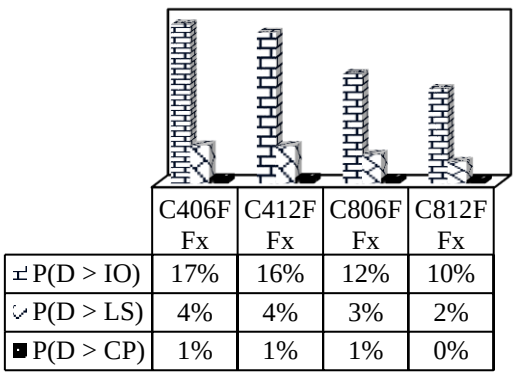

	C406F Fx	C412F Fx	C806F Fx	C812F Fx
P(D > IO)	17%	16%	12%	10%
P(D > LS)	4%	4%	3%	2%
P(D > CP)	1%	1%	1%	0%

(a)

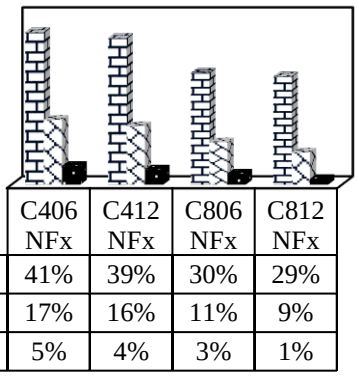

	C406 NFx	C412 NFx	C806 NFx	C812 NFx
P(D > IO)	41%	39%	30%	29%
P(D > LS)	17%	16%	11%	9%
P(D > CP)	5%	4%	3%	1%

(b)

Fig. 11. Probability of failure for different limit states subjected to an acceleration of 0.3g: a) far-field and b) near-field

According to Figure 11, the probability of experiencing extensive damage to the structures for a seismic intensity of PGA = 0.3g under near-field and far-field earthquakes such that the lives of the residents are endangered or the buildings require serious repairs, is about less than 5% and 20%, respectively.

9. Conclusions

In order to predict the seismic performance of conventional residential buildings of Qods town (located in Qom, Iran), 24 fragility curves were developed for four typical intermediate Reinforced Concrete Moment Resistant Frame structures in this area: 4 and 8 story with 1 bay, 4 and 8 story with 2 bays. They were derived through nonlinear incremental dynamic analysis in one and two horizontal directions under two sets of near-field and far-field ground motion records.

Based on the analysis results the following conclusions are drawn:

- The probability of failure for LS limit state under near-field and far-field records with a PGA of 0.3g for conventional Reinforced Concrete Moment Resistant Frame structure

located in Qods town is respectively estimated less than 5% and 20%.

- The results indicate that the seismic response of structures, which are categorized as regular according to the provisions of the 2800 standard, is the same for uni-directional and bi-directional analyses. Although 5% accidental torsion taken into account.
- Since the response of the structures with periods greater than 1 sec is in correlation with the mass-to-stiffness ratio, the damage spectrum is applicable.
- The change in the width and number of bays of the structure does not affect the probability of failure, as far as the width to the number of bays ratio is kept constant. However, the change in the height of the structure affects the probability of failure, and the shorter structures are more susceptible to damage.
- Based on the seismic response of the structures in the present study, the probability of failure is higher when the structure is subjected to near-field earthquake ground motion records.

10. References

Abdollahzadeh, G.R., Sazjini, M. and Asghari, A. (2015). "Seismic fragility Assessment of Special Truss Moment Frames (STMF) using the Capacity Spectrum Method", *Civil Engineering Infrastructures Journal*, 48(1), 1-8.

ACI 318-14. (2014). *Building code requirements for structural concrete*, American Concrete Institute, Farmington Hills, MI.

Ahmadi Pazoki, M., Shakib, H. and Mohammadi, P. (2015). "Cost-benefit analysis of construction and rehabilitation of steel braced frames with infill panels using seismic damage fragility curves", *Journal of Sharif Civil Engineering*, 31.2(1.2), 51-59.

ASCE 41-13. (2014), *Seismic evaluation and retrofit of existing buildings*, American Society of Civil Engineers, Reston, VA.

ATC-13. (1985). *Earthquake damage evaluation data for California*, Federal Emergency Management Agency (FEMA), 492 p.

Cornell, C. and Krawinkler, H. (2000). "Progress and challenges in seismic performance assessment", PEER Center News, 3, 1-3.

FEMA-356 (2000) "Prestandard and commentary for seismic rehabilitation of buildings", *Federal Emergency Management Agency*, 7(2), Washington DC.

FEMA P695. (2009). *Recommended methodology for quantification of building system performance and response parameters*, Project ATC-63, Prepared by the Applied Technology Council, Redwood City.

Building and Housing Research Center. (2016). *Iranian code of practice for seismic resistance design of buildings, Standard No. 2800, 3rd Edition*, Building and Housing Research Center, Tehran, Iran, (In Persian).

Kouhestanian, H., Pahlavan, H., Shafaei, J. and Shamekhi Amiri, M. (2019). "Probabilistic seismic assessment of RC buildings considering soft and extreme soft story irregularities subjected to main shock-aftershock sequences", *Amir Kabir Journal of Civil Engineering*, 53(2), 457-478.

Mohsenian, V., Rostamkalaee, S., Moghadam, A.S. and Beheshti-Aval, S.B., (2017). "Evaluation of seismic sensitivity of tunnel form concrete buildings to mass eccentricity in the plan", *Journal of Sharif Civil Engineering*, 33.2(3.2), 3-16.

Moehle, J. and Deierlein, G.G. (2004). "A framework methodology for performance-based earthquake engineering", *Proceedings of the 13th World Conference on Earthquake Engineering*, 679, 3812-3814.

Mobinipour, A. and Pourzeynali, S. (2020). "Assessment of near-fault ground motion effects on the fragility curves of tall steel moment resisting frames", *Civil Engineering Infrastructures Journal*, 53(1), 71-88.

Newmark, N.M. (1959). "A method of computation for structural dynamics", *Journal of Engineering Mechanics Division*, ASCE, July 67-94.

Pahlavan, H., Naseri, A. and Einolahi, A. (2019). "Probabilistic seismic vulnerability assessment of RC frame structures retrofitted with steel jacketing", *Amir Kabir Journal of Civil Engineering*, 51(3), 585-598.

Rojahn, C. and Sharpe, R.L. (1985). "Earthquake damage evaluation data for California", Applied Technology Council.

Taghizade, F., Eskandari, M., Afsari, N. and Gheitanchi, M.R. (2009). "Studying seismotectonics and seismicity of Qom province", *Earth*, 3(3), 59-70.

Whitman, R.V., Lagorio, H.J. and Schneider, P.J. (1996) "Fema- nibs earthquake loss estimation methodology", in Natural Disaster Reduction. pp. 113-114, ASCE.